Kinetics and Mechanism of the Gas-Phase Reaction of Cl Atoms with Benzene

O. Sokolov,[†] M. D. Hurley, T. J. Wallington,*[,‡] and E. W. Kaiser*

Ford Motor Company, P.O. Box 2053, Mail Drop SRL-3083, Dearborn, Michigan 48121-2053

J. Platz and O. J. Nielsen[§]

Atmospheric Chemistry, Plant Biology and Biogeochemistry Department, Risø National Laboratory, DK-4000, Roskilde, Denmark

F. Berho, M.-T. Rayez, and R. Lesclaux*[,||]

Laboratoire de Physico-Chimie Moléculaire, UMR 5803, CNRS, Université Bordeaux I, 33405 Talence - Cedex - France

Received: June 30, 1998; In Final Form: October 1, 1998

The gas-phase reaction of Cl atoms with benzene has been studied using both experimental and computational methods. The bulk of the kinetic data were obtained using steady-state photolysis of mixtures containing Cl_2, C_6H_6, and a reference compound in 120−700 Torr of N_2 diluent at 296 K. Reaction of Cl atoms with C_6H_6 proceeds via two pathways; (a) H-atom abstraction and (b) adduct formation. At 296 K the rate constant for the abstraction channel is $k_{1a} = (1.3 \pm 1.0) \times 10^{-16}$ cm^3 molecule^{-1} s^{-1}. Phenyl radicals produced via H-atom abstraction from C_6H_6 react with Cl_2 to give chlorobenzene. The main fate of the C_6H_6−Cl adduct is decomposition to reform C_6H_6 and Cl atoms. A small fraction of the C_6H_6−Cl adduct undergoes reaction with Cl atoms via a mechanism which does not lead to the production of C_6H_5Cl, or the reformation of C_6H_6. As the steady-state Cl atom concentration is increased, the fraction of the C_6H_6−Cl adduct undergoing reaction with Cl atoms increases causing an increase in the effective rate constant for benzene removal and a decrease in the chlorobenzene yield. Thermodynamic calculations show that a rapid equilibrium is established between Cl atoms, C_6H_6, and the C_6H_6−Cl adduct, and it is estimated that at 296 K the equilibrium constant is $K_{c,1b} = [C_6H_6\text{−Cl}]/[C_6H_6][Cl]$ and lies in the range $(1-2) \times 10^{-18}$ cm^3 molecule.[1] Flash photolysis experiments conducted using C_6H_6/Cl_2 mixtures in 760 Torr of either N_2 or O_2 diluent at 296 K did not reveal any significant transient UV absorption; this is entirely consistent with results from the steady-state experiments and the thermodynamic calculations. The C_6H_6−Cl adduct reacts slowly (if at all) with O_2 and an upper limit of $k(C_6H_6\text{−Cl} + O_2) < 8 \times 10^{-17}$ cm^3 molecule^{-1} s^{-1} was established. As part of this work a value of $k(Cl + CF_2ClH) = (1.7 \pm 0.1) \times 10^{-15}$ cm^3 molecule^{-1} s^{-1} was measured. These results are discussed with respect to the available literature concerning the reaction of Cl atoms with benzene.

Introduction

The reaction of Cl atoms with benzene has a long chemical history. In 1903 it was established that 1,2,3,4,5,6-hexachlorocyclohexane (HCH) was the final product of the sequence of chlorination reactions initiated by photolysis of Cl_2 in liquid benzene.[1] The first quantitative studies of the gas phase reaction were performed by Noyes and co-workers in the early 1930s[2,3] using UV irradiation of C_6H_6/Cl_2 mixtures with the course of reaction monitored via changes in total pressure. It was deduced that the reaction of chlorine atoms with benzene proceeds mainly via addition, with chlorination occurring via a short-chain mechanism (chain length of 20−50) giving HCH as the major product and chlorobenzene as a minor product.[2,3] In the late 1950s Russell and co-workers[4−7] showed that the photochlorination of organic compounds in benzene solvent proceeds via an unusual mechanism in which the active chain carrier is not the free Cl atom but is instead a weakly bound C_6H_6−Cl adduct.[5−7] The bonding in the C_6H_6−Cl adduct reduces its reactivity and increases its selectivity when compared to free Cl atoms.[8,9] In the liquid phase, the reaction of Cl atoms with benzene proceeds via addition with a rate constant of $k_1 = 1.0 \times 10^{-11}$ cm^3 molecule^{-1} s^{-1}.[10]

$$Cl + C_6H_6 \rightarrow \text{products} \qquad (1)$$

Our interest in reaction 1 stems from a desire to quantify the atmospheric chemistry and hence environmental impact of aromatic compounds released into the atmosphere by motor vehicles. In smog chamber studies of the atmospheric degradation mechanism of organic compounds it is often convenient to use Cl atoms to initiate the sequence of photooxidation reactions. To facilitate design and interpretation of such experiments, kinetic and mechanistic data concerning the reaction of Cl atoms with the aromatic compounds are needed.

There have been four published measurements of k_1 in the gas phase, all of which used relative rate techniques at ambient

* Authors to whom correspondence should be addressed.
[†] Present address: Institute of Chemical Physics, Russian Academy of Sciences, 4 Kosygin St., Moscow 117334, Russia.
[‡] E-mail: twalling@ford.com.
[§] E-mail: ole.john.nielsen@risoe.dk.
[||] E-mail: lesclaux@cribx1.u-bordeaux.fr.

10.1021/jp9828080 CCC: $15.00
Published on Web 12/04/1998

temperature in 700−740 Torr of air, or N_2, diluents. Atkinson and Aschmann monitored the loss of benzene relative to ethane following UV irradiation of $C_6H_6/C_2H_6/Cl_2$/air mixtures and derived $k_1 = (1.5 \pm 0.9) \times 10^{-11}$ cm^3 molecule^{-1} s^{-1}.[11] Relative rate studies conducted at Ford Motor Company using $C_6H_6/CH_4/Cl_2/N_2$ and $C_6H_6/CD_4/Cl_2/N_2$ mixtures did not reveal any evidence for the reaction of benzene with Cl atoms and upper limits of $k_1 < 4 \times 10^{-12}$ [12] and $k_1 < 5 \times 10^{-16}$ cm^3 molecule^{-1} s^{-1} [13] were reported. In the most recent investigation, Shi and Bernhard irradiated $C_6H_6/CF_2ClH/Cl_2$/air mixtures and from the relative loss rates of benzene and CF_2ClH derived $k_1 = (1.3 \pm 0.3) \times 10^{-15}$ cm^3 molecule^{-1} s^{-1}.[14]

Nozière et al.[13] studied the loss of benzene and methane following UV irradiation of $C_6H_6/CH_4/Cl_2$/air mixtures and reported that plots of the decay of benzene versus methane were curved, with decreasing benzene loss observed at longer irradiation times. Such behavior was attributed to complications associated with the formation of OH radicals in the system. The mechanism by which OH radicals are formed is thought to involve reaction of Cl atoms with hydroperoxides.[13] The Cl atom initiated oxidation of methane in air produces CH_3OOH which can then react with Cl atoms to give OH radicals:

$$Cl + CH_3OOH \rightarrow CH_2OOH + HCl \quad (2)$$

$$CH_2OOH \rightarrow HCHO + OH \quad (3)$$

OH radicals react more rapidly with benzene than with methane and so will preferentially attack benzene, enhancing its decay rate. As the irradiation proceeds, oxidation products build up and compete for the available OH radicals, causing the apparent decrease in the benzene reactivity observed by Nozière et al. It seems likely that a similar explanation can account for the anomalously high value of k_1 reported by Atkinson and Aschmann.[11] To avoid OH radical formation during oxidation of the reference compound, Shi and Bernhard[14] employed CF_2ClH as the reference compound. However, as discussed in the Conclusions section, it is possible that OH radicals are formed during the oxidation of benzene in air.

As noted above, it is well established that the UV irradiation of C_6H_6/Cl_2 mixtures results in a series of chlorination reactions leading to hexachlorocyclohexane (HCH). The γ-isomer of HCH is an insecticide known as Lindane, and the UV irradiation of C_6H_6/Cl_2 mixtures has been used as a commercial synthesis for this compound. In light of its commercial importance and long history of academic interest, it is very surprising that the kinetics of the reaction of Cl atoms with benzene are so poorly understood. To provide insight into this reaction we have conducted flash photolysis, relative rate, and computational studies of the kinetics and mechanism of reaction 1. As shown herein, the effective rate constant for reaction of Cl atoms with benzene in the gas phase is very small and the reaction leads to several different products. Reaction 1 is not a promising candidate for initiating the oxidation of benzene in smog chamber studies of its atmospheric oxidation mechanism.

2. Experimental Section

Relative rate and product studies were performed at Ford using FTIR-smog chamber and photochemical GC-FID systems. Absolute kinetic studies were performed at Bordeaux using a flash photolysis system described previously.[15] All quoted errors are 2 standard deviations from least-squares fits; conventional error techniques were used to propagate errors where appropriate.

2.1. Flash Photolysis System at Bordeaux. The apparatus consisted of a cylindrical reaction cell (4 cm i.d., 70 cm length). Radicals were generated by the photolysis of molecular chlorine using an argon flash lamp, surrounded by a Pyrex tube to filter out flash radiation of $\lambda < 290$ nm, preventing photodissociation of organic precursors. Molecular chlorine concentrations, $2-5 \times 10^{16}$ molecule cm^{-3}, were measured by UV absorption at 330 nm ($\sigma = 2.56 \times 10^{-19}$ cm^2 molecule^{-1}.[16]) Initial radical concentrations were $(5-10) \times 10^{13}$ molecule cm^{-3}, as calibrated by photolysis of Cl_2 in the presence of excess NO and measuring the absorption of the ClNO formed ($\sigma = 8.96 \times 10^{-18}$ cm^2 molecule^{-1} at 220 nm.[16] The analyzing light, provided by a deuterium lamp, passed through the reaction cell and was detected by a monochromator/photomultiplier unit with 2 nm band-pass. The signal was digitized by an oscilloscope and recorded and averaged with a computer for further data analyses. Kinetic parameters were derived from simulations of the complete reaction mechanism fitted to the experimental traces using nonlinear least-squares analysis. Gas mixtures were prepared using calibrated flow controllers with total replenishment of the gas mixture in the cell between each flash to avoid secondary reactions involving reaction products.

O_2, N_2, synthetic air, Cl_2 (Messer, 5% in N_2, purity > 99.9%), NO (AGA Gaz Spéciaux, 0.96% in N_2, purity > 99.9%), and CCl_4 (Prolabo, purity >99.8%) were all used without further purification. Chloroform (Acros Chimica, purity 99+%, stabilized with approximately 0.75% ethanol) was purified by distillation and storage over molecular sieves. Great care was taken in the purification of benzene (Aldrich, 99.9+ %, glass-distilled, HPLC grade).

Purification of Benzene. The degree of purification of benzene is a critical point in the determination of the rate constant $k(Cl + C_6H_6)$ in the flash photolysis experiments because the reaction was found to be very slow and the method used was equivalent to measuring the depletion of chlorine atoms (and hence is sensitive to the presence of reactive impurities). The nature of impurities was determined by GC-MS. Hydrocarbons exhibiting high reactivity with chlorine atoms, e.g., cyclohexane [$k(Cl + C_6H_{12}) = 2 \times 10^{-10}$ cm^3 molecule^{-1} s^{-1},[17]) were detected in amounts smaller than 0.15%. Simple distillation was inadequate to remove such trace impurities and a new purification method was developed. Cl_2 was dissolved in deoxygenated liquid benzene by bubbling gaseous Cl_2 (5% in nitrogen) through the sample. Chlorine atoms were generated by photolyzing Cl_2 using the radiation provided by a high-pressure mercury lamp filtered by the Pyrex vessel containing the solution. They reacted first with reactive impurities and then with benzene. This procedure converts reactive impurities and a small fraction of the benzene into chlorinated compounds which were then eliminated by distillation under a nitrogen atmosphere. Tetrachlorocyclohexene and hexachlorocyclohexane were identified among the chlorinated products, in agreement with previous studies in liquid benzene.[18,19] These two compounds were the only products produced by the above photochemical reaction, using the already purified benzene, thereby proving that they are formed by the reaction of chlorine atoms with benzene. This purification procedure proved to be very efficient; no remaining impurities (<0.01%) could be detected by GC-MS analyses.

2.2. FTIR-Smog Chamber System at Ford. A 140-liter Pyrex smog chamber interfaced to a Mattson Sirus 100 FTIR spectrometer[20] was used to study the kinetics and products of reaction 1. The reactor was surrounded by 22 fluorescent blacklamps (GE F15T8-BL). Chlorine atoms were generated

by the photolysis of molecular chlorine in 700 Torr total pressure of N_2 diluent.

$$Cl_2 + h\nu \rightarrow 2\ Cl \quad (4)$$

The concentrations of compounds were monitored by Fourier transform infrared spectroscopy using their characteristic features over the wavenumber ranges 600−700 (C_6H_6), 2180−2340 (CD_4), 1290−1330 (CF_2ClH), and 720−760 cm^{-1} (C_6H_5Cl). Infrared spectra were derived from 32 co-added interferograms (the data acquisition time was 1.5 min) using a path length of 28 m and a resolution of 0.25 cm^{-1}. Reference spectra were acquired by expanding known volumes of reference materials into the chamber. Experimental conditions for the kinetic study of reaction 1 were, 2.2−35.5 mTorr of C_6H_6, 1.1−16 mTorr of reference (either CF_2ClH or CD_4), and 14.8−2200 mTorr of Cl_2 in 700 Torr of N_2 diluent.

Four sets of experiments were performed using the FTIR-smog chamber. First, the kinetics of the reaction of Cl atoms with CF_2ClH were studied relative to CD_4. Second, the kinetics of the reaction of Cl atoms with benzene were investigated relative to the reaction of Cl atoms with CF_2ClH and CD_4. CD_4 and CF_2ClH were selected as references because their reactivities toward Cl atoms are comparable to that of benzene and because one of them, CF_2ClH, was used previously as a reference by Shi and Bernhard[14] and so facilitates comparison of the results from the present work with those reported by Shi and Bernhard. Third, the rate of reaction of Cl atoms with chlorobenzene was determined. Fourth, the products formed following the reaction of Cl atoms with C_6H_6 in N_2 diluent were investigated. All reagents used at Ford were obtained from commercial sources at research grade quality and were used without further purification.

2.3. Photochemical Reactor with Gas Chromatography Analysis at Ford. The 80 cm^3 Pyrex reactor was cylindrical, 20 cm in length, and 2.5 cm in diameter and was irradiated by a single Sylvania F6T5 BLB fluorescent lamp (1.2 cm diameter), positioned 3.3 cm from the center of the reactor. The reactants, containing CD_4, C_6H_6, Cl_2, and N_2, were premixed in a separate flask, and the reactor was filled to 120 Torr. The mixture was irradiated for a predetermined time after which the contents of the reactor were analyzed by gas chromatography using flame-ionization detection (GC-FID). The percentage consumption of C_6H_6 and CD_4 was varied by a factor of 3−6 during these experiments with no discernible impact on the measured rate constant ratios. The initial mixture contained 90 mTorr C_6H_6, 17−21 mTorr CD_4, and 0.6−17 Torr Cl_2, with the balance N_2. The initial Cl_2 density was varied to obtain different steady-state Cl atom densities in the reactor while using a constant radiative flux. An additional set of experiments using the above mixture with Cl_2 fixed at 3.1 Torr was performed in which the distance between the center of the lamp and reactor center was varied from 3.3 to 16.5 cm, causing the steady-state Cl atom density to change while keeping the mixture composition constant. As the reactor is irradiated from one side only, the steady-state Cl atom concentration will vary somewhat across the diameter of the reactor, particularly when the lamp is close, and only average Cl atom densities can be calculated in these experiments.

3. Results

3.1. Flash Photolysis Study of the Cl + C_6H_6 Reaction in the Absence of O_2. The aim of the experiments performed at Bordeaux was to identify the possible radical products of the reaction of chlorine atoms with benzene: phenyl C_6H_5 (reaction 1a), chlorocyclohexadienyl C_6H_6−Cl (reaction 1b), and cyclohexadienyl C_6H_7, resulting from channel 1c and subsequent reaction of H atoms with benzene.

$$Cl_2 + h\nu \rightarrow 2\ Cl \quad (4)$$

$$Cl + C_6H_6 \rightarrow C_6H_5 + HCl \quad (1a)$$

$$Cl + C_6H_6 \rightarrow C_6H_6{-}Cl \quad (1b)$$

$$Cl + C_6H_6 \rightarrow C_6H_5Cl + H \quad (1c)$$

Reaction enthalpies are in (units of kJ mol^{-1}): +33,[21] −30 (this work, see section 3.8), and +69[22,23] for reaction channels 1a, 1b, and 1c, respectively. Only the C_6H_6−Cl adduct, resulting from channel 1b, has a chance to be detected in flash photolysis experiments at room temperature, the other two channels being too slow as a result of their endothermicity.

Gas mixtures, $[Cl_2] = (2-5) \times 10^{16}$ and $[C_6H_6] = (2-10) \times 10^{17}$ cm^{-3} in N_2 (760 Torr), were flash-photolyzed, resulting in initial chlorine atom concentrations of (5−10) 10^{13} molecule cm^{-3}. The temperature was varied from 250 to 298 K, and the spectral region 220−330 nm was investigated to identify any transient absorption corresponding to the above radicals. The phenyl radical absorbs significantly at 250 nm ($\sigma = 2.8 \times 10^{-17}$ cm^2 $molecule^{-1}$)[24] while cyclohexadienyl radicals absorb strongly around 300 nm ($\sigma = 2.6 \times 10^{-17}$ cm^2 $molecule^{-1}$).[25]

No significant transient signals could be detected whatever the wavelength. Very weak absorptions were observed at 220 nm and between 260 and 280 nm, but they were too low (optical densities < 0.001) to be significant and probably result from some remaining impurities in benzene. Neither cyclohexadienyl nor phenyl radicals were detected, indicating that reactions 1a and 1c are too slow to be detected. In the presence of small amounts of NO (3×10^{16} molecule cm^{-3}) the well-known absorption of ClNO was observed at 220 nm ($\sigma = 8.96 \times 10^{-18}$ cm^2 $molecule^{-1}$); the addition of benzene in concentrations of up to 5×10^{17} molecule cm^{-3} had no discernible impact (<10%) on the measured ClNO absorption, showing that Cl atoms react preferentially with NO rather than with benzene. Experiments performed using CCl_4 in place of Cl_2 as the chlorine atom precursor gave the same result.

To check whether the conditions were really suitable to form cyclohexadienyl-type radicals, Cl_2/C_6H_6 mixtures were photolyzed using H_2 (700 Torr) as the carrier gas. The chemical system, forming the cyclohexadienyl radical C_6H_7, was:

$$Cl_2 + h\nu \rightarrow 2\ Cl \quad (4)$$

$$Cl + H_2 \rightarrow HCl + H \quad (5)$$

$$H + Cl_2 \rightarrow HCl + Cl \quad (6)$$

$$H + C_6H_6 \rightarrow C_6H_7 \quad (7)$$

$$Cl + C_6H_6 \rightarrow \text{products} \quad (1)$$

Reaction 5 occurs with a rate constant of 2×10^{-14} cm^3 $molecule^{-1}$ s^{-1}.[26] In the absence of benzene, a chain reaction consuming Cl_2 is initiated as observed at 330 nm by the depletion of the Cl_2 absorption. In the presence of benzene, a strong absorption was observed around 300 nm (Figure 1), consistent with the published UV spectrum of the cyclohexadienyl radical.[27] The experimental signals could be simulated by only taking into account the absorption corresponding to

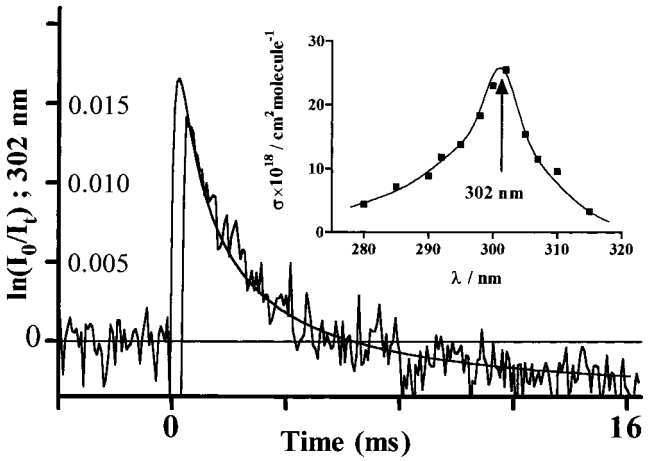

Figure 1. Typical decay trace recorded at 302 nm following flash photolysis of $Cl_2/C_6H_6/H_2$ mixtures at room temperature and atmospheric pressure. Experimental conditions: $[C_6H_6] = 3.25 \times 10^{17}$, $[H_2] = 2.5 \times 10^{19}$, $[Cl_2] = 1 \times 10^{16}$, leading to $[C_6H_7]_0 = 2.5 \times 10^{13}$ (units of molecule cm^{-3}); the solid line is a simulation of the data. Negative values of $\ln(I_o/I_t)$ at longer reaction times arise from Cl_2 depletion (see text for details). The insert shows the UV absorption spectrum of the C_6H_7 radical.

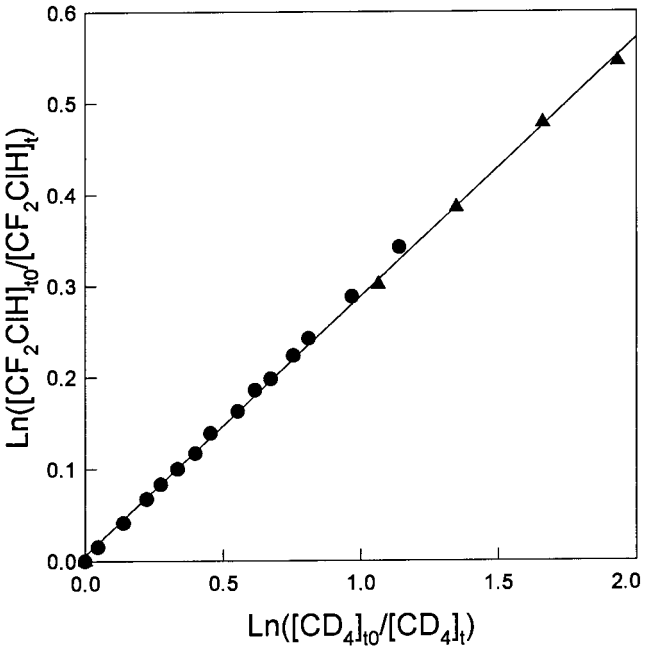

Figure 2. Decay of CF_2ClH versus CD_4 when mixtures containing these compounds were exposed to Cl atoms in 700 Torr total pressure of N_2 at 296 K. Circles were obtained using mixtures of $[Cl_2] = 46$ mTorr, $[CF_2ClH] = 7$ mTorr, and $[CD_4] = 18$ mTorr. Triangles were obtained using mixtures of $[Cl_2] = 2.07$ Torr, $[CF_2ClH] = 7$ mTorr, $[CD_4] = 16$ mTorr, and $[C_6H_6] = 3.7$ mTorr.

cyclohexadienyl radicals (with $\sigma = 2.6 \times 10^{-17}$ cm^2 $molecule^{-1}$ at 302 nm[25]) without considering the reaction of Cl atoms with benzene.

From the flash photolysis experiments, it can be concluded that the reaction Cl + C_6H_6 is either very slow, which was expected for channels 1a and 1c or equilibrated (equilibrium largely shifted toward the reactants) so that chlorine atoms remain available to react irreversibly with NO and H_2. This is certainly the case for the addition pathway (reaction 1b), as the rate constant for addition is expected to be large. Theoretical calculations failed to find any barrier on the addition pathway (see section 3.8), and thus a rate constant value between 10^{-12} cm^3 $molecule^{-1}$ s^{-1} (as for OH + benzene[13]) and 10^{-11} cm^3 $molecule^{-1}$ s^{-1}, as observed in the liquid phase,[10] is expected. Assuming that the C_6H_6−Cl radical behaves like other cyclohexadienyl radicals and absorbs around 300 nm with an absorption section of $\sigma \approx 10^{-17}$ cm^2 $molecule^{-1}$,[28] we can derive an order of magnitude estimate for the upper limit of $K_{c,1b} < 10^{-18}$ cm^3 $molecule^{-1}$ from the flash photolysis experiments.

3.2. Relative Rate Study of k(Cl + CF_2ClH). Prior to the FTIR study of reaction 1, experiments were performed to measure the reactivity of Cl atoms toward CF_2ClH. A relative rate method was used to measure k_8 relative to k_9 using the 140 liter FTIR−smog chamber at Ford. The experimental techniques are described elsewhere.[29]

$$Cl + CF_2ClH \rightarrow \text{products} \quad (8)$$

$$Cl + CD_4 \rightarrow \text{products} \quad (9)$$

Control experiments were performed to check for complications caused by photolysis, heterogeneous loss, and reaction of Cl_2 with CF_2ClH and CD_4; no evidence for such complications was observed. The experimental conditions used to measure k_8/k_9 were $[Cl_2] = 46$ mTorr, $[CF_2ClH] = 7$ mTorr, $[CD_4] = 18$ mTorr, in 700 Torr of N_2 diluent at 296 K. The observed loss of CF_2ClH versus that of CD_4 following UV irradiation of $CF_2ClH/CD_4/Cl_2/N_2$ mixtures is shown in Figure 2. The triangles in Figure 2 are data obtained in the presence of benzene (see section 3.3 for details). Linear least-squares analysis of the data in Figure 2 gives $k_8/k_9 = 0.28 \pm 0.02$. Using $k_9 = 6.1 \times 10^{-15}$ [29] gives $k_8 = (1.7 \pm 0.1) \times 10^{-15}$ cm^3 $molecule^{-1}$ s^{-1}. This result is consistent with previous measurements of $k_8 = 2.0 \times 10^{-15}$ [30] and $k_8 = 1.7 \times 10^{-15}$ cm^3 $molecule^{-1}$ s^{-1},[31] providing confidence in the experimental procedures used herein.

3.3. Relative Rate Study of the Cl + C_6H_6 Reaction in 700 Torr of N_2. Relative rate studies were performed using the FTIR-smog chamber and photochemical reactor GC-FID systems at Ford. The loss of C_6H_6 was monitored relative to that of CF_2ClH or CD_4 following the UV irradiation of $C_6H_6/CF_2ClH/Cl_2/N_2$ and $C_6H_6/CD_4/Cl_2/N_2$ mixtures. The experimental conditions used are given in sections 2.2 and 2.3. Control experiments were performed to check for complications caused by photolysis, heterogeneous loss, and reaction of Cl_2 with C_6H_6, CF_2ClH, and CD_4; no evidence for such complications was observed. Typical data showing the observed loss of C_6H_6 versus CD_4 following UV irradiation of $C_6H_6/CD_4/Cl_2/N_2$ mixtures in the FTIR-smog chamber are given in the insert in Figure 3B. Variation of the initial molecular chlorine concentration, UV irradiation intensity, and initial reactant concentrations had no systematic effect on the values of k_1/k_8 and k_1/k_9 obtained (providing $[Cl]_{ss}$ does not change). Interestingly, however, the measured values of k_1/k_8 and k_1/k_9 varied in a systematic fashion with changes in the Cl atom steady-state concentration in the individual experiments. The steady-state Cl atom concentration, $[Cl]_{ss}$, was calculated from the observed rate of decay of the reference compounds (CF_2ClH or CD_4) using the expression:

$$[Cl]_{ss} = \left(\frac{1}{t \times k_{ref}}\right) \mathrm{Ln}\left(\frac{[\text{Reference}]_{to}}{[\text{Reference}]_t}\right)$$

where t is the time of irradiation time in seconds, k_{ref} is the reference rate constant (k_8 or k_9), and $[\text{Reference}]_{to}$ and $[\text{Reference}]_t$ are the concentrations of the reference compound before and after the irradiation. The assumptions inherent in the use of this expression are the following: (i) the reference compounds are lost solely via reaction with Cl atoms and are

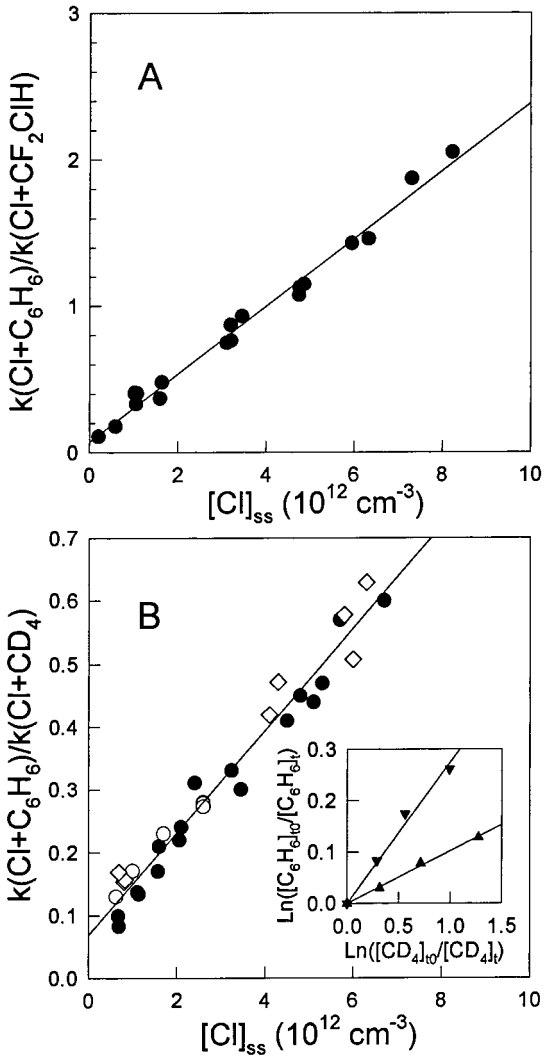

Figure 3. Effective rate constant for the reaction of Cl atoms with C_6H_6 measured relative to the rate constants for reaction of Cl atoms with CF_2ClH (A) and CD_4 (B) plotted versus the steady-state Cl atom concentration in experiments in 700 Torr total pressure of N_2 at 296 K. Open symbols were obtained using the GC-FID apparatus at 120 Torr, closed symbols with the FTIR system at 700 Torr. The diamonds show results obtained using a constant light intensity with varying $[Cl_2]$; open circles show results obtained at a constant $[Cl_2]$ with the light intensity varied. The insert in panel B shows the observed loss of C_6H_6 versus that of CD_4 following the UV irradiation of a mixtures of 3.7 mTorr of C_6H_6, 11.1 mTorr of CD_4, and 204 mTorr of Cl_2 (triangles) and 3.8 mTorr of C_6H_6, 10.9 mTorr of CD_4, and 2 Torr of Cl_2 (inverted triangles) in 700 Torr of N_2 diluent in the FTIR-smog chamber.

not reformed in any process, (ii) the values used for k_{ref} are accurate, (iii) the UV light source provides a constant illumination of the reaction mixtures, (iv) the lifetime of Cl atoms is short compared to the irradiation time, and (υ) the $[Cl]_{ss}$ is constant throughout the irradiation period. Let us consider these assumptions in turn.

First it is not difficult to conceive of reactions by which benzene or the reference compounds are lost which do not involve Cl atoms, e.g.,

$$C_6H_5 + CF_2ClH \rightarrow C_6H_6 + CF_2Cl \quad (10)$$

$$CF_2Cl + C_6H_6 \rightarrow \text{products} \quad (11)$$

To test for loss of CF_2ClH or CD_4 via reactions with products from reaction 1 experiments were performed using a $C_6H_6/CF_2ClH/CD_4/Cl_2/N_2$ mixture with $[C_6H_6] = 3.70$ mTorr, $[Cl_2] = 2.07$ Torr, $[CF_2ClH] = 7.55$ mTorr, and $[CD_4] = 15.5$ mTorr, in 700 Torr of N_2 diluent at 296 K. As shown by the triangles in Figure 2, the relative decay rates of CF_2ClH and CD_4 were not impacted by the presence of benzene or its reaction products. As a test for possible complications caused by reaction of benzene with products from reaction 8, experiments were performed using comparable $[Cl]_{ss}$ values with $[CF_2ClH]$ varied by a factor of 7. There was no discernible effect of $[CF_2ClH]$ on the measured value of k_1/k_8. We conclude that the first assumption is valid.

Second, the results presented in section 3.2 suggest that the values used for k_{ref} are accurate. Third, fluorescent blacklamps were used as the UV source; typical periods of UV illumination were 1−15 min. Prior to their use the UV lamps were switched on for 10 min to "warm". It seems reasonable to assume that the output of the lamps does not change greatly during the course of an experiment. Fourth, for the concentrations of reactants used in the present work it can be calculated that the Cl atom lifetime is at least 2 orders of magnitude less than the UV irradiation times. Fifth, the measured $[Cl]_{ss}$ did not change appreciably (<10%) with the amount of the reactants consumed. All assumptions inherent in the calculation of $[Cl]_{ss}$ seem reasonable.

Figure 3A,B shows the measured values of k_1/k_8 and k_1/k_9 plotted versus $[Cl]_{ss}$ for both FTIR and GC-FID experiments. As seen from Figure 3 the apparent reactivity of Cl atoms toward benzene increases linearly with the steady-state Cl atom concentration. The results from both the GC and FTIR experiments fall on the same line even though the initial reactant concentrations for these two techniques are very different (FTIR conditions were: $[CD_4]_o = 5.2-11.4$ mTorr, $[C_6H_6] = 2.2-3.7$ mTorr, $[Cl_2] = 0.044-2.0$ Torr, GC conditions were: $[CD_4]_o = 17-21$ mTorr, $[C_6H_6] = 90$ mTorr, $[Cl_2] = 0.6-17$ Torr). This provides strong support for ascribing this effect to the Cl atom concentration rather than to any of the initial reactant concentrations such as Cl_2.

The plots in Figure 3A,B have positive *y*-axis intercepts. The simplest explanation for the behavior shown in Figure 3 is to postulate that reaction of Cl atoms with benzene proceeds via two channels: H-atom abstraction and addition to give a C_6H_6-Cl adduct which can either undergo decomposition back to reactants, or react further with Cl atoms in a manner that does not regenerate benzene.

$$Cl + C_6H_6 \rightarrow C_6H_5 + HCl \quad (1a)$$

$$Cl + C_6H_6 \rightarrow C_6H_6-Cl \quad (1b)$$

$$C_6H_6-Cl \rightarrow Cl + C_6H_6 \quad (-1b)$$

$$C_6H_6-Cl + Cl \rightarrow \text{products} \quad (12a)$$

Because of the substantial endothermicity of reaction 1c, it is ignored in the above mechanism. It is possible, even likely, that some fraction of the reaction of Cl atoms with the C_6H_6-Cl adduct proceeds to regenerate C_6H_6 and Cl_2 which then constitutes benzene-catalyzed recombination of Cl atoms.

$$C_6H_6-Cl + Cl \rightarrow C_6H_6 + Cl_2 \quad (12b)$$

The relevant differential equations are

$$-d[C_6H_6]/dt = k_{1a}[Cl][C_6H_6] + k_{1b}[Cl][C_6H_6] - k_{-1b}[C_6H_6-Cl] - k_{12b}[C_6H_6-Cl][Cl]$$

$$d[C_6H_6{-}Cl]/dt = k_{1b}[Cl][C_6H_6] - k_{-1b}[C_6H_6{-}Cl] - k_{12}[C_6H_6{-}Cl][Cl]$$

where $k_{12} = (k_{12a} + k_{12b})$.

Application of the steady-state approximation for the $[C_6H_6{-}Cl]$ adduct gives

$$-d[C_6H_6]/dt = k_{1a}[Cl]_{ss}[C_6H_6] + k_{1b}k_{12a}[Cl]_{ss}^2[C_6H_6]/(k_{-1b}+k_{12}[Cl]_{ss})$$

In our experiments we measure an effective rate constant for reaction 1 given by

$$-d[C_6H_6]/dt = k_{eff}[Cl]_{ss}[C_6H_6]$$

hence $k_{eff} = k_{1a} + k_{1b}k_{12a}[Cl]_{ss}/(k_{-1b} + k_{12}[Cl]_{ss})$.

We can consider two extreme behaviors depending on the relative magnitudes of k_{-1b} and $k_{12}[Cl]_{ss}$. When $k_{12}[Cl]_{ss} \gg k_{-1b}$ the expression reduces to $k_{eff} = k_{1a} + k_{1b}k_{12a}/k_{12}$ and no dependence on the Cl atom steady-state concentration will be observed. When $k_{12}[Cl]_{ss} \ll k_{-1b}$ the effective rate constant will have a linear dependence on [Cl] and k_{eff} is given by

$$k_{eff} = k_{1a} + (k_{1b}k_{12a}[Cl]_{ss})/k_{-1b}$$

As seen from Figure 3, the experimental observations show a linear dependence of k_{eff} on the Cl atom concentration which is consistent with the simple model above with decomposition via reaction −1b being the dominant fate of the $C_6H_6{-}Cl$ adduct. The data in Figure 3B using CD_4 reference were obtained from experiments conducted in both the 140 liter FTIR-smog chamber facility (filled symbols) and the 80 cm^3 photochemical reactor − GC-FID system (opened symbols). Indistinguishable results were obtained in the two systems. In both experimental systems variation of $[Cl]_{ss}$ was achieved by either maintaining a given UV intensity and varying $[Cl_2]$ or by keeping $[Cl_2]$ constant and varying the UV intensity (see sections 2.2 and 2.3 for details). This is illustrated by the GC-FID data in Figure 3B. This figure shows rate constant ratios obtained with the same initial reaction mixture but with different light intensity (open circles) as described in section 2.3. This changes the $[Cl]_{ss}$ as expected. Also shown are data at constant light intensity but differing $[Cl_2]$ (open diamonds). The method by which the $[Cl]_{ss}$ was varied had no discernible effect on the measured value of k_{eff}.

Linear least-squares analysis of the data in Figure 3A gives an intercept $= k_{1a}/k_8 = 0.0737 \pm 0.0560$ and a slope $= (k_{1b}k_{12a})/(k_{-1b}k_8) = (0.231 \pm 0.023) \times 10^{-12}$ cm^3 $molecule^{-1}$, using $k_8 = (1.7 \pm 0.1) \times 10^{-15}$ cm^3 $molecule^{-1}$ s^{-1} gives $k_{1a} = (1.3 \pm 1.0) \times 10^{-16}$ cm^3 $molecule^{-1}$ s^{-1} and $(k_{1b}k_{12a})/(k_{-1b}) = (3.9 \pm 0.5) \times 10^{-28}$ cm^6 $molecule^{-2}$ s^{-1}. Similar analysis of the data in Figure 3B gives an intercept $= k_{1a}/k_9 = 0.0688 \pm 0.0402$ and a slope $= (k_{1b}k_{12a})/(k_{-1b}\ k_9) = (0.0813 \pm 0.0080) \times 10^{-12}$ cm^3 $molecule^{-1}$. Using $k_9 = 6.1 \times 10^{-15}$ cm^3 $molecule^{-1}$ s^{-1} [29] gives $k_{1a} = (4.2 \pm 2.4) \times 10^{-16}$ cm^3 $molecule^{-1}$ s^{-1} and $(k_{1b}k_{12a})/(k_{-1b}) = (4.9 \pm 0.5) \times 10^{-28}$ cm^6 $molecule^{-2}$ s^{-1}. Within the admittedly large uncertainties (particularly for the intercept), consistent data are obtained from experiments using the two different reference compounds. As seen in Figure 3 the data obtained using CD_4 as reference are more scattered than those obtained using CF_2ClH. This extra scatter reflects the inherent difficulties associated with measurement of rate constant ratios which deviate markedly from unity. Data were collected using CF_2ClH as reference at lower values of $[Cl]_{ss}$ which provides a more accurate determination of k_{1a}. Accordingly, we choose to quote final values of $k_{1a} = (1.3 \pm 1.0) \times 10^{-16}$ cm^3 $molecule^{-1}$ s^{-1} based upon the CF_2ClH data and $(k_{1b}k_{12a})/(k_{-1b}) = (4.5 \pm 1.1) \times 10^{-28}$ cm^6 $molecule^{-2}$ s^{-1} (average from CF_2ClH and CD_4 experiments).

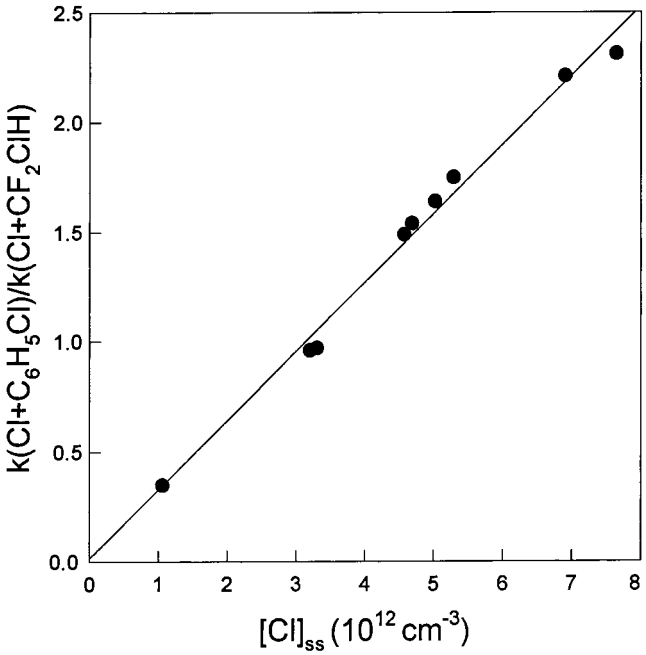

Figure 4. Effective rate constant for the reaction of Cl atoms with C_6H_5Cl measured relative to the reaction of Cl atoms with CF_2ClH plotted versus the steady-state Cl atom concentration in experiments in 700 Torr total pressure of N_2 at 296 K.

We can use the measured value of $(k_{1b}k_{12a})/(k_{-1b})$ to provide an estimate of the equilibrium constant $K_{c,1b} = k_{1b}/k_{-1b}$. By comparison with reactions of other alkyl radicals with Cl atoms[32] it seems likely that reaction 12a proceeds with a rate constant which is close to the gas kinetic limit, i.e., $k_{12a} = (2{-}4) \times 10^{-10}$ cm^3 $molecule^{-1}$ s^{-1}. Hence, we estimate $K_{c,1b} = k_{1b}/k_{-1b} = (1{-}2) \times 10^{-18}$ cm^3 $molecule^{-1}$. This result is consistent with the conclusion from the flash photolysis experiments (section 3.1) that $K_{c,1b}$ is of the order of 1×10^{-18} cm^3 $molecule^{-1}$ or less.

Reaction 1a is endothermic by 33 kJ mol^{-1}.[21] The calculations presented in section 3.8 show that this reaction proceeds with an activation barrier close to the reaction endothermicity. We can use the value of k_{1a} measured above to arrive at a preexponential A factor of 6×10^{-11} cm^3 $molecule^{-1}$ s^{-1}. This result is very reasonable for hydrogen abstraction by Cl atoms which typically have A factors of $1{-}10 \times 10^{-11}$ cm^3 $molecule^{-1}$ s^{-1}.[16]

3.4. Relative Rate Study of the Cl + C_6H_5Cl Reaction in 700 Torr of N_2. Prior to a product study of reaction 1, experiments were performed using the FTIR-smog chamber system to measure the kinetics of reaction 13 relative to reaction 8.

$$Cl + C_6H_5Cl \rightarrow \text{products} \quad (13)$$

$$CF_2ClH + Cl \rightarrow \text{products} \quad (8)$$

As with the reaction of Cl atoms with benzene, the effective rate constant for reaction of Cl atoms with chlorobenzene increased with the steady-state chlorine atom concentration. Figure 4 shows a plot of the measured values of k_{13}/k_8 versus $[Cl]_{ss}$. As discussed in the previous section, the simplest chemical mechanism that can explain the observed behavior is

$$Cl + C_6H_5Cl \rightarrow C_6H_4Cl + HCl \quad (13a)$$

$$Cl + C_6H_5Cl \rightarrow C_6H_5Cl{-}Cl \quad (13b)$$

$$C_6H_5Cl{-}Cl + Cl \rightarrow \text{products} \quad (14a)$$

$$C_6H_5Cl{-}Cl + Cl \rightarrow C_6H_5Cl + Cl_2 \quad (14b)$$

Linear least-squares analysis of the data in Figure 4 gives an intercept $= k_{13a}/k_8 = 0.015 \pm 0.120$ and a slope $= (k_{13b}k_{14a})/(k_{-13b}k_8) = (0.31 \pm 0.03) \times 10^{-12}$ molecule^{-1} cm^3, using $k_8 = (1.7 \pm 0.1) \times 10^{-15}$ cm^3 molecule^{-1} s^{-1} gives $k_{13a} < 2.5 \times 10^{-16}$ cm^3 molecule^{-1} s^{-1} and $(k_{13b}k_{14a})/(k_{-13b}) = (5.3 \pm 0.6) \times 10^{-28}$ cm^6 molecule^{-2} s^{-1}. Within the experimental uncertainties, there is no evidence for a direct bimolecular component of the reaction of Cl atoms with chlorobenzene.

3.5. Study of the Products Formed Following the UV Irradiation of $Cl_2/C_6H_6/N_2$ Mixtures. To provide insight into the mechanism of the reaction of Cl atoms with benzene, experiments were performed to determine the products following UV irradiation of $Cl_2/C_6H_6/N_2$ mixtures using the FTIR-smog chamber facility. Figure 5 shows typical IR spectra obtained before (A) and after (B) a 2 min irradiation of a mixture of 2.6 Torr of Cl_2 and 36.4 mTorr of C_6H_6 in 700 Torr of N_2 at 296 K. Comparison of the features in panel B with the reference spectrum of chlorobenzene given in panel C clearly shows the formation of chlorobenzene. Chlorobenzene was observed as a product in all experiments. The insert in Figure 6 shows the formation of chlorobenzene versus loss of benzene following irradiation of a mixture containing 38.5 mTorr of Cl_2, 30.6 mTorr of C_6H_6, and 1.18 mTorr of CF_2ClH in 700 Torr of N_2. Subtraction of IR features attributable to benzene and chlorobenzene from panel B gives the residual IR features at 743, 794, 827, 894, 997, and 1020 cm^{-1} shown in panel D. We are unable to identify the product(s) responsible for these residual features. Likely candidates for the unknown product(s) include various isomers of dichlorocyclohexadiene, tetrachlorocyclohexene, and hexachlorocyclohexane. In the absence of authentic samples of these compounds which we can introduce into the chamber we are unable to establish their yields. Small corrections were applied to account for loss of chlorobenzene via reaction 13. As seen from Figure 6, the yield of chlorobenzene varied inversely with the Cl atom steady-state concentration. The following simple model was used to rationalize the kinetic data in section 3.3.

$$Cl + C_6H_6 \rightarrow C_6H_5 + HCl \quad (1a)$$

$$Cl + C_6H_6 \rightarrow C_6H_6{-}Cl \quad (1b)$$

$$C_6H_6{-}Cl \rightarrow Cl + C_6H_6 \quad (-1b)$$

$$C_6H_6{-}Cl + Cl \rightarrow \text{products} \quad (12)$$

The phenyl radicals produced in reaction 1a are expected to react rapidly with Cl_2 to give chlorobenzene.

$$C_6H_5 + Cl_2 \rightarrow C_6H_5Cl + Cl \quad (15)$$

If we assume that all phenyl radicals react via reaction 15 and that there are no other sources of chlorobenzene, then its molar yield should be given by

$$k_{1a}/k_{\text{eff}} = k_{1a}/\{k_{1a} + (k_{1b}k_{12a}[Cl])/k_{-1b}\}$$

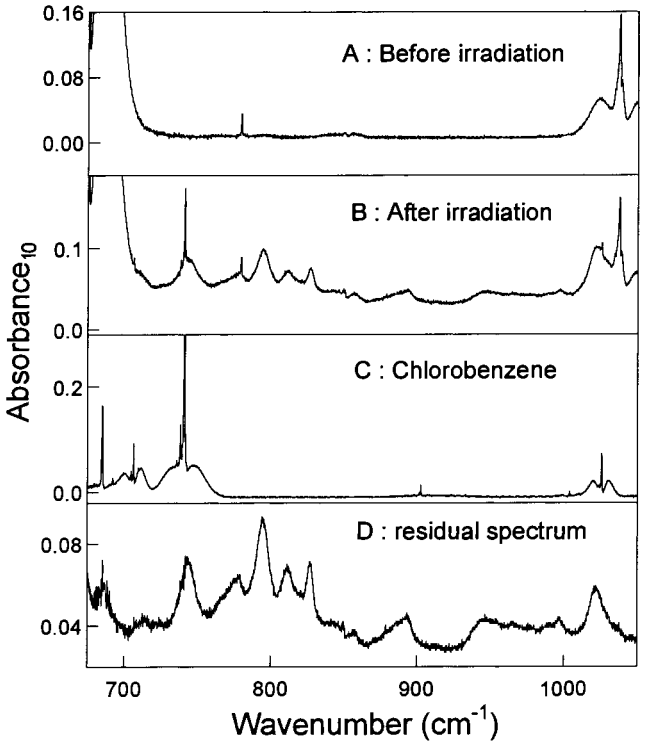

Figure 5. IR spectra obtained before (A) and after (B) a 2 min irradiation of a mixture of 2.6 Torr of Cl_2 and 36.4 mTorr of C_6H_6 in 700 Torr of N_2 at 296 K. Panel C is a reference spectrum of chlorobenzene. Unidentified product features obtained by subtraction of features attributable to C_6H_6 and chlorobenzene from panel B are shown in panel D.

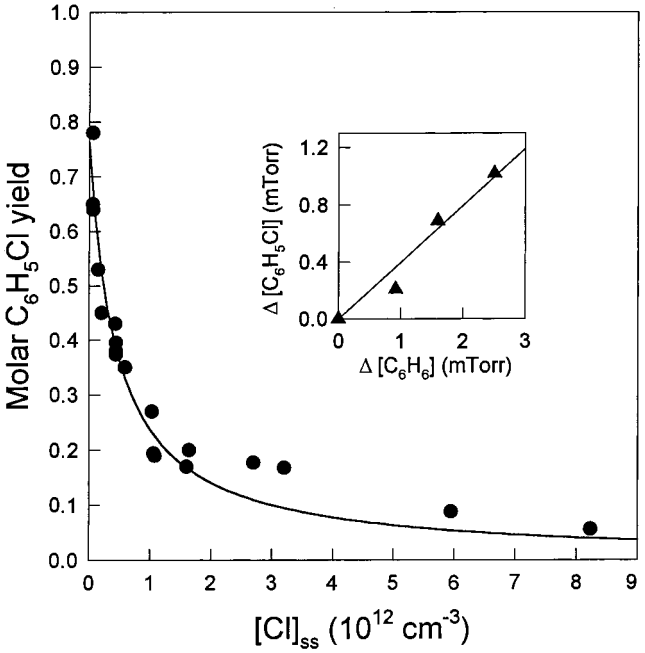

Figure 6. Yield of chlorobenzene following UV irradiation of $C_6H_6/Cl_2/N_2$ mixtures plotted versus the steady-state Cl atom concentration. The insert shows the observed increase in chlorobenzene versus loss of C_6H_6 following UV irradiation of a mixture of 30.6 mTorr of C_6H_6, 1.18 mTorr of CF_2ClH, and 38.5 mTorr of Cl_2, in 700 Torr of N_2 diluent, the steady-state Cl atom concentration calculated for this experiment was 0.44×10^{12} cm^{-3}.

Consistent with the experimental observations shown in Figure 6, the above expression predicts that the yield of chlorobenzene will vary inversely with the Cl atom steady-state concentration. The simple model given above predicts that as

$[Cl]_{ss}$ increases, the yield of chlorobenzene should tend toward zero which is consistent with the data given in Figure 6. Also the model predicts that as $[Cl]_{ss}$ approaches zero the chlorobenzene yield should approach unity. Experimentally we observe that the chlorobenzene yield increases with decreasing $[Cl]_{ss}$ but does not appear to quite reach unity. The largest chlorobenzene yield was 78%. There are three possible explanations for the apparent 22% shortfall in the chlorobenzene yield at the lowest values of $[Cl]_{ss}$. First, the simple model above could be deficient in a small loss of the C_6H_6-Cl adduct which is not dependent on Cl atoms and which does not lead to chlorobenzene product. Second, the model could be deficient in a loss of phenyl radicals other than reaction 15. Third, there could be a systematic calibration error in our measurement of the chlorobenzene yield or a systematic underestimation of $[Cl]_{ss}$. With regard to the second point, on the basis of the database for other alkyl radicals[32] it seems reasonable to assume that reaction 15 proceeds with a rate constant of the order of 10^{-11} cm^3 molecule^{-1} s^{-1} and in the presence of 0.015−2.0 Torr of Cl_2 it is difficult to imagine any competing loss mechanisms for phenyl radicals. We estimate that possible systematic errors associated with calibrations of the reference spectra of benzene and chlorobenzene together contribute a 15% uncertainty in measurement of the chlorobenzene yield. After subtraction of the chlorobenzene features from the product spectra obtained in experiments using high values of $[Cl]_{ss}$, residual IR features attributed to one or more unknown product(s) were observed. These residual features decrease progressively for experiments with lower values of $[Cl]_{ss}$. At the very lowest $[Cl]_{ss}$ there are no discernible residual features after subtraction of those belonging to benzene and chlorobenzene. We cannot exclude the possibility that an undetected product is formed at the 10−20% yield level in experiments conducted at the lowest $[Cl]_{ss}$ conditions. However, we do not have any evidence for such a complication and for simplicity we will proceed on the assumption that the apparent shortfall in the chlorobenzene reflects a calibration error. Rearranging the expression given above for k_{1a}/k_{eff} and including an arbitrary calibration factor "CF" we can derive:

$$\text{chlorobenzene yield} = \text{CF} \times 1/\{1 + (k_{1b}k_{12a}[Cl])/(k_{-1b}k_{1a})\}$$

The smooth curve in Figure 6 shows a fit of the above expression to the data which gives CF = 0.76 ± 0.10 and $(k_{1b}k_{12a})/(k_{-1b}k_{1a}) = (2.2 \pm 0.9) \times 10^{-12}$ cm^3 molecule^{-1}. This result can be combined with the value of $(k_{1b}k_{12a})/(k_{-1b}) = (4.5 \pm 1.1) \times 10^{-28}$ cm^6 molecule^{-2} s^{-1} from section 3.3 to give $k_{1a} = (2.0 \pm 1.0) \times 10^{-16}$ cm^3 molecule^{-1} s^{-1} which is consistent with the value of $k_{1a} = (1.3 \pm 1.0) \times 10^{-16}$ cm^3 molecule^{-1} s^{-1} derived from the intercept in Figure 3A. It is gratifying to note that the simple model of the Cl-atom-initiated chlorination of benzene presented in section 3.3 provides a self-consistent qualitative and quantitative explanation of both the observed kinetic behavior and product distribution of the system.

3.6. Flash Photolysis Study of the Cl + C_6H_6 Reaction in the Presence of O_2. In the presence of excess oxygen, transient signals could be observed at wavelengths between 220 and 290 nm. However, these signals were very low in intensity and were at the detection limit of the system (approximately 0.2% absorption), and the corresponding absorption spectrum did not exhibit any well-characterized maximum. Despite some similarity of the spectrum with those generally observed for peroxy radicals, no information about the nature of the products of the reaction could be derived from these absorption signals (they cannot be assigned to the $C_6H_5O_2$ radical since no phenyl radicals could be observed in the absence of oxygen). These observations might be consistent with a reaction of the C_6H_6-Cl adduct with O_2, alternatively the observed transient signals might be due to the reaction of chlorine atoms with remaining impurities in the benzene sample (0.01% would be enough).

Because of the equilibrium of the addition pathway (reactions 1b, −1b), it is difficult to measure the rate constant of the addition reaction of Cl atoms with C_6H_6 (k_{1b}). In principle, this should be possible provided the adduct can be readily eliminated by reaction with a radical scavenger such as O_2. We have attempted to measure the rate constant k_{1b} in the presence of a large excess of oxygen, using a relative method, the reference reaction being Cl + $CHCl_3$. It is well-known that chloroform is oxidized into phosgene via a chain reaction.[33] The reaction of Cl atoms with benzene was used as a termination of the chain reaction and the rate constant was derived from simulations of the time-resolved phosgene build-up signals at 240 nm, for different benzene concentrations. The result was $k_1 = (9.8 \pm 4.1) \times 10^{-15}$ cm^3 molecule^{-1} s^{-1}, using $k(Cl + CHCl_3) = (1.1 \pm 0.4) \times 10^{-13}$ cm^3 molecule^{-1} s^{-1} at 298 K.[17] However, the rate constant value was found unchanged when the oxygen concentration was decreased to values as low as 10^{17} molecule cm^{-3}, which is totally inconsistent with the value of the equilibrium constant estimated in sections 3.1 and 3.3. For the lowest O_2 concentrations, it would require the rate constant value for the reaction of the adduct with O_2 to be larger than the gas kinetic limit. We conclude that the measured rate constant cannot be that of the addition channel. Because of the possible presence of remaining impurities in benzene it rather corresponds to an upper limit of the overall rate constant, in agreement with other results reported in this paper. This result implies that even in the presence of 700 Torr of O_2, any reaction between the C_6H_6-Cl adduct and O_2 is slow.

3.7. Relative Rate Study of the Cl + C_6H_6 Reaction in 700 Torr of Air. To provide insight into the reactions occurring during the Cl-atom-initiated oxidation of benzene in air and to provide a direct comparison with the previous study of Shi and Bernhard,[14] relative rate experiments were performed to measure k_1/k_8 in 700 Torr of air diluent at 296 K. Two reaction mixtures were used with initial concentration ratios $[C_6H_6]_o/[CF_2ClH]_o$ chosen to be comparable to those employed by Shi and Bernhard.[14] Figure 7 shows the observed loss of C_6H_6 versus that of CF_2ClH following UV irradiation of $C_6H_6/CF_2ClH/Cl_2$/air mixtures (for initial conditions see figure caption). As seen from Figure 7, variation of $[C_6H_6]_o/[CF_2ClH]_o$ by a factor of 6 had no discernible effect on the relative decay rates of C_6H_6 and CF_2ClH. The relative rate plot in Figure 7 shows modest but significant curvature. The line in Figure 7 is a linear fit to the first 6 data points which gives a slope of 0.71 which is similar to the value of $k_1/k_8 = 0.757 \pm 0.024$ reported by Shi and Bernhard.[14] The curvature in Figure 7 indicates that either reactions 1 and 8 are not the sole loss mechanisms for C_6H_6 and CF_2ClH, or that there are processes that regenerate C_6H_6 or CF_2ClH. In the presence of 700 Torr of air it is difficult to imagine reactions that regenerate C_6H_6 or CF_2ClH. We believe that the most likely explanation for the observed curvature lies in the generation of OH radicals during the Cl-atom-initiated oxidation of C_6H_6. OH radicals react 300 times faster with benzene than with CF_2ClH,[16,34] and their generation will lead to an enhanced rate of benzene loss. As reaction products build up there will be a competition for the available OH radicals, resulting in decreased benzene loss and curvature in the relative rate plot. From the rate of CF_2ClH loss the $[Cl]_{ss}$ is calculated

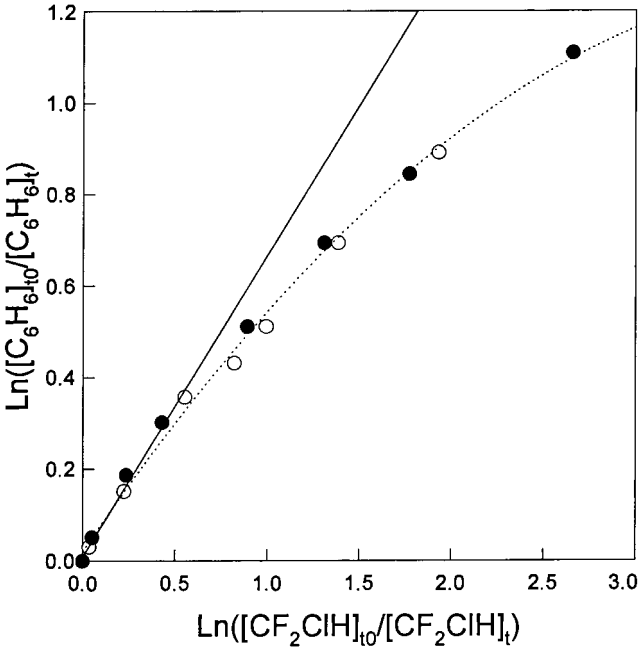

Figure 7. Decay of C_6H_6 versus CF_2ClH when mixtures containing these compounds were exposed to Cl atoms in 700 Torr total pressure of *air* at 296 K. Open symbols were obtained using mixtures of $[Cl_2] = 370$ mTorr, $[CF_2ClH] = 7.4$ mTorr, and $[C_6H_6] = 4.4$ mTorr. Filled symbols were obtained using mixtures of $[Cl_2] = 370$ mTorr, $[CF_2ClH] = 4$ mTorr, and $[C_6H_6] = 15$ mTorr.

to be 8×10^{11} cm^{-3}, by reference to Figure 3A it can be seen that at this steady-state Cl atom concentration a value of $k_1/k_8 = 0.3$ is expected from the "pure" Cl atom reactions. The initial rate of C_6H_6 loss observed in experiments conducted in 700 Torr of air is 2.5 times that expected on the basis of the results obtained in N_2 diluent. It is worth noting that the slope of the relative rate plot in Figure 7 at high consumptions of CF_2ClH and C_6H_6 tends toward the value of $k_1/k_8 = 0.3$ expected from the "pure" Cl atom reactions. This behavior can be rationalized in terms of loss of OH radicals via reaction with benzene oxidation products.

Chlorobenzene was observed as a minor product (molar yield of 6−8%) in the relative rate experiments described above. The origin of the chlorobenzene product observed in experiments conducted in N_2 diluent (see section 3.4) is reaction 1a followed by reaction 15:

$$Cl + C_6H_6 \rightarrow C_6H_5 + HCl \quad (1a)$$

$$Cl + C_6H_6 \rightarrow C_6H_6{-}Cl \quad (1b)$$

$$C_6H_5 + Cl_2 \rightarrow C_6H_5Cl + Cl \quad (15)$$

In the presence of O_2 the phenyl radicals produced in reaction 1a will be efficiently scavenged via reaction 16.[35]

$$C_6H_5 + O_2 + M \rightarrow C_6H_5O_2 + M \quad (16)$$

The mechanism by which chlorobenzene is formed in the experiments conducted in air is different from that operative in N_2 diluent. One possible explanation is that O_2 reacts with the $C_6H_6{-}Cl$ adduct:

$$C_6H_6{-}Cl + O_2 \rightarrow C_6H_5Cl + HO_2 \quad (17a)$$

$$C_6H_6{-}Cl + O_2 \rightarrow \text{products other than } C_6H_5Cl + HO_2 \quad (17b)$$

The effect of reaction 17 is to augment the loss of benzene, and this reaction may contribute to the "enhanced" loss of benzene observed in experiments conducted in air diluent. The yield of chlorobenzene was small (6−8%) and any contribution by reaction 17a is correspondingly small. It can be argued that the reaction of the $C_6H_6{-}Cl$ adduct with O_2 proceeds via more than one reaction channel and so makes a larger contribution to the "enhanced" benzene loss. While this may be true there are two points to bear in mind when discussing the potential importance of reaction 17. First, the O_2 concentration is constant and any enhanced rate of benzene loss would be constant during the experiment. The experimental results shown in Figure 7 show a decrease in the rate of benzene loss for longer irradiations; thus reaction of the $C_6H_6{-}Cl$ adduct with O_2 cannot solely explain the experimental observations. Second, in absolute terms, any "enhancement" caused by reaction of the $C_6H_6{-}Cl$ adduct with O_2 is modest. An upper limit for k_{17}, $(k_{17a} + k_{17b})$, can be derived by applying the following logic. As discussed above, the initial rate of benzene loss in 700 Torr air is 2.5 times that expected for the "pure" Cl atom reactions. In the experiments described above in 700 Torr of air the concentration of O_2 was $4.8 \times 10^{18}/8 \times 10^{11} = 5.9 \times 10^6$ times greater than that of Cl atoms. Ascribing the entire enhanced benzene loss to reaction of the adduct with O_2, it follows that a factor of 5.9×10^6 excess of O_2 over Cl atoms increases the benzene loss by an additional 150%. Reaction 12a cannot proceed faster than the gas kinetic limit, $k_{12a} < 3 \times 10^{-10}$, hence $k_{17} < 8 \times 10^{-17}$ cm^3 molecule^{-1} s^{-1}. It is clear that reaction of the $C_6H_6{-}Cl$ adduct with O_2 occurs slowly (if at all).

To provide insight into the dependence of the C_6H_5Cl yield on the O_2 concentration, six experiments were performed using mixtures of 50 mTorr of C_6H_6, 2 mTorr of CF_2ClH, 100 or 500 mTorr of Cl_2, and 10, 147, or 700 Torr of O_2 in 700 Torr total pressure made up with N_2 diluent as appropriate. The results are given in Table 1. The molar yields of C_6H_5Cl were small. The $[Cl]_{ss}$ concentrations were calculated from the observed loss rate of the CF_2ClH tracer. The increase in the C_6H_5Cl yield with increasing $[O_2]$ for the experiments conducted using $[Cl_2] = 100$ mTorr, although small, was significant and since $[O_2]$ was the only parameter that was changed significantly it seems reasonable to speculate that reaction 17a makes a small contribution. It should be stressed that the magnitude of the sensitivity of the C_6H_5Cl yield to a 70-fold change in $[O_2]$ is very small and that even in the presence of 700 Torr of O_2, any role played by reaction 17a is minor. The reactions occurring during the Cl-initiated oxidation of benzene in the presence of O_2 are complex and poorly characterized. The aim of the present work was to elucidate the kinetics of the reaction of Cl atoms with benzene, not the detailed chemistry associated with the subsequent reactions in air diluent. Experiments in N_2/O_2 diluent were not pursued further.

Unlike our data shown in Figure 7, Shi and Bernhard[14] observed linear behavior in their relative rate plots. Furthermore, in apparent contrast to our results, Shi and Bernhard[14] report that "no significant C_6H_5Cl was observed in the C_6H_6/Cl_2/air system despite extensive efforts for its identification by FTIR spectroscopy". The origin of the different behavior observed in the two studies is unclear.

Theoretical Calculations. The value of the equilibrium constant, $K_{c,1b}$, of the addition channel is a critical parameter for interpreting the present results. Experimental results can provide rough estimates of the $K_{c,1b}$ value, but we have found it important to assess the consistency of these estimated values with the thermochemical parameters that can be derived from

TABLE 1: Molar Yields of C_6H_5Cl Observed Following the UV Irradiation of Mixtures of 50 mTorr of C_6H_6, 2 mTorr of CF_2ClH (added as a Cl atom tracer), and 100 or 500 mTorr of Cl_2 in N_2/O_2 Diluent at 700 Torr Total Pressure and 296 K

	O_2 (Torr)		
Cl_2 (mTorr)	10	147	700
100	$Y(C_6H_5Cl) = 3.9\%$ $[Cl]_{ss} = 3.6 \times 10^{11}$ cm^{-3}	$Y(C_6H_5Cl) = 5.2\%$ $[Cl]_{ss} = 3.1 \times 10^{11}$ cm^{-3}	$Y(C_6H_5Cl) = 6.3\%$ $[Cl]_{ss} = 3.0 \times 10^{11}$ cm^{-3}
500	$Y(C_6H_5Cl) = 6.3\%$ $[Cl]_{ss} = 1.0 \times 10^{12}$ cm^{-3}	$Y(C_6H_5Cl) = 6.4\%$ $[Cl]_{ss} = 8.0 \times 10^{11}$ cm^{-3}	$Y(C_6H_5Cl) = 9.8\%$ $[Cl]_{ss} = 6.0 \times 10^{11}$ cm^{-3}

TABLE 2: Calculated and Experimental Thermochemical Parameters of the Cl + C_6H_6 Reaction; the Parameters for the Addition Channel of H and OH to C_6H_6 Are Included for Comparison

	calculated (BAC-MP4)		experimental
	ΔH°_{298} (kJ mol^{-1})	ΔS°_{298} (J mol^{-1} K^{-1})	ΔH°_{298} (kJ mol^{-1})
$Cl + C_6H_6 \rightarrow HCl + C_6H_5$ (1a)	+48	*a*	+33[b]
$Cl + C_6H_6 \rightarrow C_6H_6{-}Cl$ (1b)	−30	−92	*a*
$Cl + C_6H_6 \rightarrow H + C_6H_5Cl$ (1c)	+60	*a*	+69[b]
$H + C_6H_6 \rightarrow C_6H_7$	−79	−89	−92[c]
$OH + C_6H_6 \rightarrow C_6H_6{-}OH$	−74	−112	−69[d]

[a] Not determined. [b] Refs 21 and 22. [c] Ref 28. [d] Ref 40.

quantum calculations. For comparison calculations were also performed to characterize the adducts of H atoms and OH radicals with benzene.

The heats of formation of the different compounds involved in this study were calculated using the Melius BAC-MP4 method. Stationary points were fully optimized at the HF/6-31G(d) level of theory using the GAUSSIAN94 package of programs. Vibrational frequencies were systematically scaled down by a factor of 0.89, and thermochemical parameters were calculated. Electronic correlation was taken into account by performing MP4(SDTQ) single-point calculations using the 6-31G(d,p) basis set. In a second step, the Melius BAC program[36−38] improves the energetical results by empirical corrections using bond−additivity approximations accounting for the systematic errors resulting mainly from basis set truncation. Additional corrections for electron-spin contamination, related to open-shell and/or unsaturated systems, are also included.

For the species involved in channels 1a and 1c, the values of the heats of formation, calculated using the same method, were directly taken from Melius' results.[36−38] The reaction enthalpies calculated for each reaction pathway 1a, 1b, and 1c are reported in Table 2 along with the corresponding experimental values for channels 1a and 1c, taken from thermochemical tables.[22,23] We were unable to characterize any stable π-adduct between Cl atoms and C_6H_6; the bonding in such a π-adduct is less than 12 kJ mol^{-1}. The π-adduct cannot survive more than a few picoseconds at ambient temperature and is too short-lived to play any role in the chemical system. The thermodynamic results shown for reaction 1b in Table 2 are for the σ-adduct.

Despite a difference of 15 kJ mol^{-1} between the calculated and the experimental values for the hydrogen abstraction channel, the calculations are consistent with the measured endothermicity of channels 1a and 1c. This is consistent with the low rate constant measured for the hydrogen abstraction reaction. Given the substantial endothermicity of channel 1c this channel can be ignored. Channel 1b is calculated to be exothermic by 30 kJ mol^{-1} with an estimated uncertainty of ±10 kJ mol^{-1}; this result is consistent with the value of $\Delta H^\circ_{298} = -33$ kJ mol^{-1} reported by Ritter et al.[39] The equilibrium constant, derived from the thermochemical parameters given in Table 1 lies in the range:

$$K_{c,1b} = 10^{-17} - 10^{-21} \text{ cm}^3 \text{ molecule}^{-1} \text{ at } 298 \text{ K}$$

confirming that the equilibrium is largely shifted toward the reactants at room temperature. The flash photolysis experiments described in section 3.1 suggest that $K_{c,1b}$ is of the order of 10^{-18} cm^3 molecule^{-1}, or less. The FTIR experiments described in section 3.3 suggest that $K_{c,1b}$ lies in the range $(1-2) \times 10^{-18}$ cm^3 molecule^{-1}. It is gratifying that the experimental and computational results are consistent. Based upon the FTIR results we conclude that $K_{c,1b}$ lies in the range $(1-2) \times 10^{-18}$ cm^3 molecule^{-1}.

Calculations were also performed to search for a possible barrier for the addition pathway. As the Cl atom approaches the benzene molecule the energy of the system was always lower than the energy of the separated reactants. The same result was obtained using other ab initio (DFT) or semiempirical (AM1) methods; there is no barrier on the addition pathway (channel 1b). This finding is consistent with the high rate constant (10^{-11} cm^3 molecule^{-1} s^{-1}) found for this reaction channel in liquid benzene.[10] Similar calculations were performed to search for a barrier on the hydrogen abstraction pathway (1a); none was found.

As shown in Table 2, the chlorocyclohexadienyl radical is much less stable than cyclohexadienyl and hydroxycyclohexadienyl radicals, all values being calculated using the same method. The values for the cyclohexadienyl and hydroxycyclohexadienyl radicals given in Table 2 are consistent with the experimentally measured parameters,[25,40] providing confidence that the thermochemical data reported in Table 2 are reliable.

4. Conclusions

A large and self-consistent body of experimental data is presented which suggests that the gas-phase reaction of Cl atoms with benzene proceeds via two channels: H atom abstraction and $C_6H_6{-}Cl$ adduct formation. The rate of the abstraction channel, $k_{1a} = (1.3 \pm 1.0) \times 10^{-16}$ cm^3 molecule^{-1} s^{-1}, is consistent with that expected on the basis of thermochemical arguments assuming the activation energy is equal to the reaction endothermicity (see section 3.8). In the liquid-phase reaction, it has been established that addition of Cl atoms to benzene to give the $C_6H_6{-}Cl$ adduct proceeds rapidly with a rate constant of 1.0×10^{-11} cm^3 molecule^{-1} s^{-1}.[10] In view of the size of the adduct and the presence of 700 Torr of N_2 diluent in the present experiments it seems likely that the addition channel (1b) will be close to the high-pressure limit and k_{1b} will be comparable to that measured in the liquid-phase studies. Combining an estimate of $k_{1b} = 1.0 \times 10^{-11}$ cm^3 molecule^{-1} s^{-1} with the fact that the effective overall rate constant k_{eff} for reaction 1 observed here is of the order of $10^{-16}-10^{-15}$ cm^3 molecule^{-1} s^{-1}, it must be concluded that the overwhelming fate of the $C_6H_6{-}Cl$ adduct under the present experimental conditions is decomposition back to reactants. As discussed in section 3.2, the linearity of the data in Figure 3A,B is also consistent with $k_{-1b} \gg k_{12}[Cl]_{ss}$.

We show here that the C_6H_6−Cl adduct reacts with Cl atoms. From the fact that the chlorobenzene yield tends to zero at high $[Cl]_{ss}$ (see Figure 6), we conclude that this reaction does not produce C_6H_5Cl. At this point the germane question is "What is the likely nature of the reaction of Cl atoms with the adduct?" Two products are possible: dichlorocyclohexadiene, or a di-adduct in which two Cl atoms are bound to the same benzene molecule. Chemical intuition suggests that the former is more likely.

At room temperature there is a rapid equilibrium between Cl atoms and the C_6H_6−Cl adduct, the equilibrium being largely shifted toward the reactants. Results from experiments and calculations provide a consistent picture of the instability of the chlorocyclohexadienyl radical, $\Delta H_{decomp} = 30-33$ kJ mol^{-1}, corresponding to $k_{-1b} = 10^7$ s^{-1} at room temperature. From a combination of experimental results and quantum calculations, we estimate that $K_{c,1b} = k_{1b}/k_{-1b} \approx (1-2) \times 10^{-18}$ cm^3 molecule^{-1}.

The low value of the equilibrium constant indicates that, even with the high benzene concentrations used in flash photolysis experiments, the equilibrium is shifted toward the reactants to a sufficient extent for preventing any transient absorption corresponding to the chlorocyclohexadienyl radical from being detected. As far as FTIR experiments are concerned, the low value of both the equilibrium constant and rate constant for hydrogen abstraction results in fairly high steady-state concentrations of Cl atoms, thus allowing a fraction of the C_6H_6−Cl radicals to be scavenged through the fast reaction with Cl atoms. This results in the determination of effective rate constants and product yields which both depend on experimental conditions. This partly explains the discrepancies observed in the literature concerning this reaction (see Introduction).

In the presence of oxygen, the effective rate constant has also been found to be very slow. In this case, discrepancies may also arise from the formation of the OH radical in the oxidation process, as already mentioned in the Introduction. It was initially thought that the C_6H_6−Cl adduct could be scavenged by the addition of a large excess of oxygen. It is shown in this work that this is not the case. Reaction between the adduct and oxygen proceeds slowly (if at all) and an upper limit of $k(C_6H_6\text{−Cl} + O_2) < 8 \times 10^{-17}$ cm^3 molecule^{-1} s^{-1} was established (see section 3.7).

Low reactivity of the C_6H_6−Cl adduct with O_2 has been observed in the liquid phase by Skell et al.[41] These authors report a much lower reactivity of the C_6H_6−Cl radical with O_2, than that of the C_6H_7 radical, which corroborates the trend observed here in the gas phase, since a rate constant of 4×10^{-14} cm^3 molecule^{-1} s^{-1} has been determined recently[25] for the $C_6H_7 + O_2$ reaction. In addition, a low rate constant, $<2 \times 10^{-16}$ cm^3 molecule^{-1} s^{-1}, has also been reported for the C_6H_6−OH + O_2 reaction.[42] The low reactivity of cyclohexadienyl-type radicals presumably reflects their high resonance stabilization energy (100 kJ mol^{-1} for C_6H_7)[43].

The effective rate constant for reaction of Cl atoms with benzene in the gas phase is very small and the reaction leads to several different products. Reaction 1 is not a promising candidate for initiating the oxidation of benzene in smog chamber studies of its atmospheric oxidation mechanism.

Acknowledgment. F.B., M.T.R., and R.L. thank Daniel Liotard (Université Bordeaux I) for performing semiempirical calculations and the French Ministry of Environment for financial support.

References and Notes

(1) Slator, A. *Z. Physik. Chem.* **1903**, *45*, 540.

(2) Lane, C. E., Jr.; Noyes, W. A., Jr. *J. Am. Chem. Soc.* **1932**, *54*, 161.

(3) Smith, H. P.; Noyes, W. A., Jr.; Hart, E. J. *J. Am. Chem. Soc.* **1933**, *55*, 4444.

(4) Russell, G. A.; Brown, H. C. *J. Am. Chem. Soc.* **1955**, *77*, 4031.

(5) Russell, G. A. *J. Am. Chem. Soc.* **1957**, *79*, 2977.

(6) Russell, G. A. *J. Am. Chem. Soc.* **1958**, *80*, 4987.

(7) Russell, G. A. *J. Am. Chem. Soc.* **1958**, *80*, 4997.

(8) Skell, P. S.; Baxter, H. N., III; Taylor, C. K. *J. Am. Chem. Soc.* **1983**, *105*, 120.

(9) Benson, S. W. *J. Am. Chem. Soc.* **1993**, *115*, 6969.

(10) Bunce, N. J.; Ingold, K. U.; Landers, J. P.; Lusztyk, J.; Scaiano, J. C. *J. Am. Chem. Soc.* **1985**, *107*, 5464.

(11) Atkinson, R.; Aschmann, S. M. *Int. J. Chem. Kinet.* **1985**, *17*, 33.

(12) Wallington, T. J.; Skewes, L. M.; Siegl, W. O. *J. Photochem. Photobiol. A: Chem.* **1988**, *45*, 167.

(13) Nozière, B.; Lesclaux, R.; Hurley, M. D.; Dearth, M. A.; Wallington, T. J. *J. Phys. Chem.* **1994**, *98*, 2864.

(14) Shi, J.; Bernhard, M. J. *Int. J. Chem. Kinet.* **1997**, *29*, 349.

(15) Lightfoot, P. D.; Lesclaux, R.; Veyret, B. *J. Phys. Chem.* **1990**, *94*, 700.

(16) DeMore, W. B.; Sander, S. P.; Golden, D. M.; Hampson, R. F.; Kurylo, M. J.; Howard, C. J.; Ravishankara, A. R.; Kolb, C. E.; Molina, M. J. Jet Propulsion Laboratory Publication 97-4, Pasadena, CA, 1997.

(17) Rowley, D. M.; Lesclaux, R.; Lightfoot, P. D.; Noziere, B.; Wallington, T. J.; Hurley, M. D. *J. Phys. Chem.* **1992**, *96*, 4889.

(18) *Methods in free radical chemistry*, Vol 1; Poutsma, M. L., Huyser E. S., Eds.; Marcel Dekker: New York, 1969.

(19) Walling C. *Free radicals in solution*; Wiley: New York, 1957.

(20) Wallington, T. J.; Japar, S. M. *J. Atmos. Chem.* **1989**, *9*, 399.

(21) Stein, S. E.; Rukkers, J. M.; Brown, R. L. NIST Standard Reference Database 25, Gaithersburg, MD, 1991.

(22) Chase, M. W., Jr.; Davies, C. A.; Downey, J. R., Jr.; Frurip, D. J.; McDonald, R. A.; Syveruid, A. N. *J. Phys. Chem. Ref. Data* **1985**, *14*, 718, 743, and 1211.

(23) Lias, S. G.; Bartmess, J. E.; Liebman, J. F.; Holmes, J. L.; Levin, R. D.; Mallard, W. G. *J. Phys. Chem. Ref. Data* **1988**, *17*, 225, 226, and 231.

(24) Wallington, T. J.; Egsgaard, H.; Nielsen, O. J.; Platz, J.; Sehested, J.; Stein, T. *Chem. Phys. Lett.* **1998**, *290*, 363.

(25) Berho, F.; Rayez, M.-T.; Lesclaux, R. *J. Phys. Chem A.*, submitted for publication.

(26) Ackermann, L.; Hippler, H.; Pagsberg, P.; Reihs, C.; Troe, J. *J. Phys. Chem.* **1990**, *94*, 5247.

(27) Sauer, M. C., Jr.; Ward, B. *J. Phys. Chem.* **1967**, *71*, 3971.

(28) Sauer, M.; Mani, I. *J. Phys. Chem.* **1970**, *74*, 59.

(29) Wallington, T. J.; Hurley, M. D. *Chem. Phys. Lett.* **1992**, *189*, 437.

(30) Tuazon, E. C.; Atkinson, R.; Corchnoy, S. B. *Int. J. Chem. Kinet.* **1992**, *24*, 639.

(31) Sawerysyn, J. P.; Talhaoui, A.; Meriaux, B.; Devolder, P. *Chem. Phys. Lett.* **1992**, *198*, 197.

(32) Westley, F.; Frizzell, D. H.; Herron, J. T.; Hampson, R. F.; Mallard, W. G. NIST Chemical Kinetics Database Version 6.01, Gaithersburg, MD, 1994.

(33) Catoire, V.; Lesclaux, R. *J. Phys. Chem.* **1996**, *100*, 14356.

(34) Atkinson, R. *J. Phys. Chem. Ref. Data* **1989**, Monograph No. 1.

(35) Yu, T.; Lin, M. C. *J. Am. Chem. Soc.* **1994**, *116*, 9571.

(36) Melius, C. F.; Binkley, J. S. 20th Symposium (Intl) on Combustion; The Combustion Institute, Pittsburgh, 575, 1984.

(37) Melius, C. F. In *Chemistry and Physics of Energetic Materials*, NATO SAI 309, Bulusu, S. N., Ed.; Kluwer Academic: The Netherlands, **1990**; p 21.

(38) Ho, P.; Melius, C. F. *J. Phys. Chem.* **1990**, *94*, 5120.

(39) Ritter, E. R.; Bozzelli, J. W.; Dean, A. M. *J. Phys. Chem.* **1990**, *94*, 2493.

(40) Witte, F.; Urbanik, E.; Zetzsch, C. *J. Phys. Chem.* **1986**, *90*, 3251.

(41) Skell, P. S.; Baxter, H. N., III; Tanko, J. M.; Chebolu, V. *J. Am. Chem. Soc.* **1986**, *108*, 6300.

(42) Knispel, R.; Koch, R.; Siese, M.; Zetzsch, C. *Ber. Bunsen-Ges. Phys. Chem.* **1990**, *94*, 1375.

(43) Egger, K. W.; Benson, S. W. *J. Am. Chem. Soc.* **1966**, *88*, 241.